International Journal of GEOMATE
(Geotechnique, Construction Materials and Environment)
ISSN: 2186-2982 (P), 2186-2990 (O), Japan

Vol. 31, Issue 143, July, 2026, pp.138-146; DOI: 10.21660/2026.143.5437

# NUMERICAL ANALYSIS OF INNOVATIVE PRECAST CONCRETE COLUMN MORTISE-TENON SPLICE UNDER LATERAL LOAD

*Daniel Christianto[1], Andrew Hartanto Jusuf[2], Sunarjo Leman[3], Yenny Untari Liucius[4] and Tavio[5]

[1,3,4]Civil Engineering Study Program, Tarumanagara University, Indonesia;
[2,5]Department of Civil Engineering, Institut Teknologi Sepuluh Nopember, Indonesia

*Corresponding Author, Received: 16 Jan. 2026, Revised: 24 Feb. 2026, Accepted: 10 Mar. 2026

**ABSTRACT:** A previous shaking table test of an 8-story miniature precast concrete moment frame building with non-emulative dowel-based connections yielded favorable results. To upscale these connections, a mortise-tenon concept using a concrete-filled steel pipe has been proposed to replace the dowels in column splices. Although a design procedure has been developed, further numerical analysis is required to confirm it and to predict the experimental behavior. This study presents the first numerical investigation of this connection type and serves as a pre-experimental analysis to guide future experimental studies. This study focuses on finite element analysis of a 450 mm × 450 mm × 3000 mm cantilever precast concrete column with a mortise-tenon splice utilizing a Ø130 mm × 20 mm × 1200 mm concrete-filled steel pipe under monotonic lateral loading, compared with a monolithic column. The pipe centroid is located at 1 m from the fixed base, coinciding with the column segment interface. Results show that the precast column has a similar load-displacement curve shape to the monolithic column but with reduced capacity due to localized stress at the connection interface. At a 25 mm top column displacement, the precast column achieves 88.28 kN lateral capacity and 25,600 kNm/rad secant rotational stiffness at the connection. The design procedure yields a conservative factored capacity of 60.95 kN (69% of finite element analysis results), confirming its suitability for proportioning test specimens. The observed concentrated damage at the connection emphasizes the need for further full-scale cyclic experimental validation for seismic design recommendations.

*Keywords: Column splice, Concrete-filled steel pipe, Monotonic lateral load, Mortise-tenon, Precast concrete*

## 1. INTRODUCTION

With the advancement of concrete construction technology, the increasing demand for high-rise buildings due to limited available land, and the increasing efforts to reduce environmental damage, environmentally friendly high-strength concrete has become a major focus in current concrete material research. Such concrete often requires special materials or methods that are still relatively seldom used in conventional concrete construction or cast-in-place construction, such as elimination of coarse aggregates [1-4], addition of marble powders [5] and steel fibers [6-7], and substitution of cement with waste materials [8]. In order to ensure the quality and properties of environmentally friendly high-strength concrete, precast concrete will be more preferred and used more often. In precast concrete construction, structural members, such as beams, columns, and slabs, are manufactured in a factory before being assembled on the construction site [9]. This method makes the construction time of precast concrete construction much shorter compared to conventional concrete construction [10]. Furthermore, precast concrete is also suitable for sustainable development because the environmental impact of concrete production can be more effectively controlled in the factory [11].

The connections of precast concrete structural members that utilize cast-in-place concrete and are detailed similarly to monolithic concrete construction are called monolithic emulative connections [10]. The design of these emulative connections must comply with ACI 318M-19 [12]. To maximize the advantages of precast concrete, the use of cast-in-place concrete in the connections of precast concrete members must be minimized. Such precast concrete connections are called non-emulative connections and mainly utilize steel plates, bolts, weld, rubber, grout, or similar components [13-20]. However, non-emulative connections are highly varied and do not behave the same as monolithic concrete structures, so testing in accordance with ACI 374.1-05 [13] is essential, especially in earthquake-prone regions like Indonesia.

Other than experimental validation, numerical studies play a crucial role in developing innovative

construction systems, such as non-emulative precast concrete connections. Finite element analysis allows researchers to predict structural behavior, identify deficiencies, and optimize detailing before costly laboratory testing. Siswosukarto et al. [21] validated finite element models against experiments on GFRP-confined concrete, accurately capturing confinement effects and failure patterns with 2–5 times increased deformation capacity. Sandjaya et al. [22] developed finite element models for cold-formed steel plates under pure shear, revealing post-buckling stress distributions that traditional theory fails to capture while achieving good correlation with experimental tests. Similarly, Akhmad and Tavio [23] used ABAQUS to simulate long-term seawater degradation of GFRP-strengthened beams, predicting 11–21% load capacity reductions over 12–48 months without years of experimental exposure.

Various types of non-emulative precast concrete column splice connections have been researched experimentally and numerically. Hansapinyo et al. [14] demonstrated that steel box connections at column bases could achieve 1.16–1.24 times the capacity of monolithic columns when properly detailed, but crucially identified that improper welding led to brittle failures. Around the same time, Nzabonimpa and Hong [15] pioneered detachable high-yield metal plates for column splices, showing that 26 mm thick plates provided sufficient stiffness, though plates placed too close to the base caused premature concrete degradation. Building on this, Nguyen and Hong [16] introduced interior bolts and rib stiffeners, finding that stiffened plates achieved up to 159% flexural capacity increase compared to unstiffened plates, far exceeding the 24% gain from simply using higher-strength steel. These studies established that steel-based connections can match or exceed monolithic performance, but all rely on either field welding or complex bolting arrangements.

Inspired from timber structures, Yan and Jiang [17] adapted mortise-tenon concepts to precast columns using steel plate connectors with welded reinforcement, achieving 83–94% of monolithic capacity with superior ductility (11–27% higher). However, weld fracture in thin plates led to minimum 6 mm thickness recommendations, reinforcing earlier concerns from Hansapinyo et al [14] about weld quality. In contrast, Prasetya and Tavio [18] proposed a fundamentally different approach: a bolted-steel box dry joint designed to remain elastic while plastic hinges form in beams, demonstrating that bolt-only connections could eliminate field welding entirely while maintaining seismic performance.

Other researchers have also explored mortise-tenon concept for precast connections. Zhu et al. [19] extended the mortise-tenon concept to beam-column joints, showing through finite element analysis that mortise-tenon joints exhibited less damage than cast-in-place counterparts with yield loads up to 38% higher. Wang et al. [20] addressed the residual drift limitations of pure mortise-tenon joints by combining unbonded prestressed strands with mortise-tenon connections, demonstrating that prestressing mitigates cumulative slip damage.

Parallel to these advances, a shaking table test of a miniature 8-story precast concrete moment frame building with non-emulative beam-to-column and column connections utilizing steel dowels in a mortise-tenon configuration demonstrated excellent seismic performance of the structure [24]. For application in full-scale buildings, these connections need to be modified, upscaled, and tested in accordance with applicable regulations [13]. Jusuf et al. [24] proposed replacing the steel dowels with concrete-filled steel pipe as the tenon element, addressing the size limitations of dowels for actual construction. By modifying the model of Osanai et al. [25], Jusuf et al. [24] developed a rational design procedure for precast column mortise-tenon splices utilizing concrete-filled steel pipe and also provided detailed connection examples for a 3-story precast concrete moment frame building, as shown in Figure 1.

While these studies have progressively refined non-emulative connections for precast concrete, most of them require either extensive field welding, grouting, or post-tensioning. The method proposed by Jusuf et al. [24] offers a potential solution by eliminating field welding through a concrete-filled steel pipe tenon, but their design procedure has not yet been verified through numerical or experimental testing under monotonic or cyclic loads. Since experimental testing requires considerable time and cost, finite element analysis can provide an initial understanding of connection behavior and identify potential deficiencies before laboratory testing commences. The present study represents the first numerical investigation of a mortise-tenon splice for precast concrete columns utilizing concrete-filled steel pipe, serving as a pre-experimental analysis to validate the design procedure from Jusuf et al. [24]. As a pre-experimental analysis, its primary purpose is to identify potential deficiencies in the connection detailing and the rational design procedure before proceeding to costly laboratory testing.

Using the connection details provided by Jusuf et al. [24], a precast concrete column with mortise-tenon splice that utilize concrete-filled steel pipe is analyzed under monotonic lateral loading.

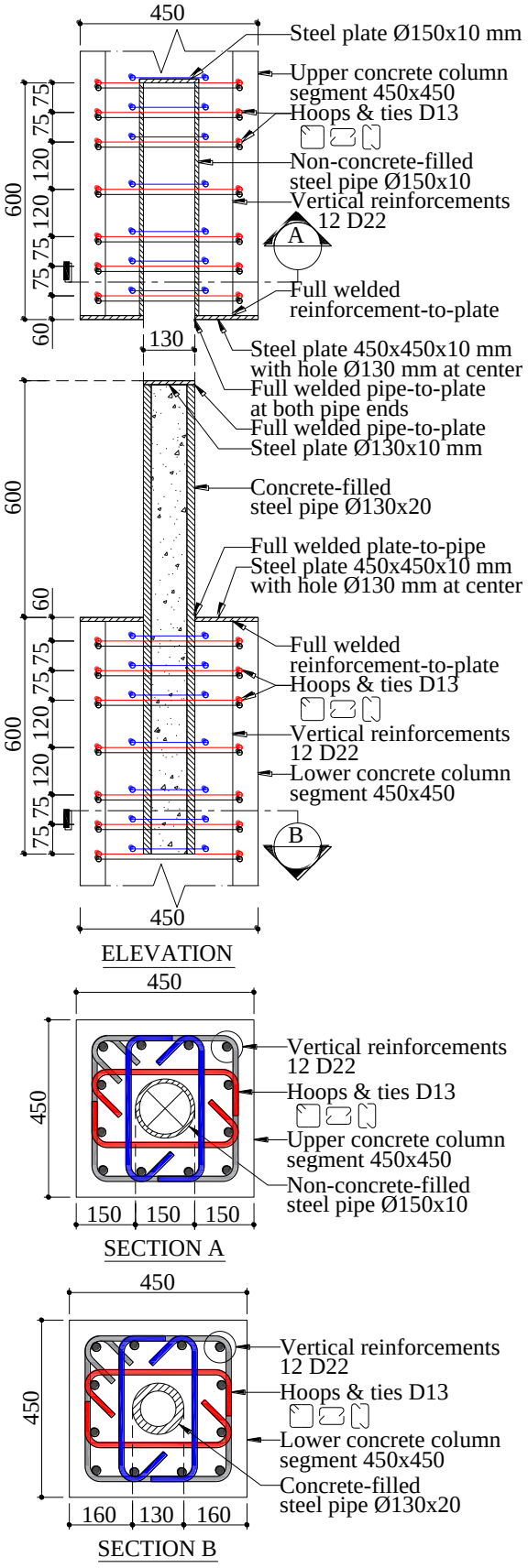


Fig.1 Example detail of precast concrete column mortise-tenon splice [24]

The results, including crack patterns, steel stresses, load-displacement behavior, and moment-rotation response, are evaluated against the design procedure. These results are compared with a monolithic column to assess structural performance and identify potential detailing improvements before experimental testing.

The research significance is presented next, highlighting the novel contributions of this numerical study and its role as a pre-experimental investigation. The finite element modeling approach used in this study is then described, including material properties, element types, boundary conditions, and loading protocol. Results are subsequently presented and discussed, covering crack patterns, stress distributions in reinforcement and steel pipe, load-displacement behavior, and moment-rotation response of the connection. Finally, key findings are summarized, the design procedure is validated against numerical results, limitations of the current study are acknowledged, and recommendations for future experimental research are provided.

## 2. RESEARCH SIGNIFICANCE

This study presents the first numerical investigation of a precast concrete mortise-tenon splice utilizing concrete-filled steel pipe to provide critical pre-experimental insights into the connection behavior. This study confirms that the design procedure from Jusuf et al. [24] yields conservative capacity estimates suitable for proportioning test specimens per code requirements [12-13]. Beyond design validation, this study identifies localized stress concentrations and damage mechanisms not previously understood. The rotational stiffness values reported offer preliminary design targets for engineers. These findings directly inform future experimental studies and demonstrate the potential of mortise-tenon concept for non-emulative precast concrete columns connections.

## 3. METHOD

The finite element analysis of the precast concrete column mortise-tenon splice utilizing concrete-filled steel pipe was performed using the MIDAS FEA NX 2024 v1.1 software. The finite element model for the precast concrete column was created based on the connection details from Jusuf et al. [24] as shown in Figure 1. A 450 mm × 450 mm × 3000 mm cantilever column was modeled using solid elements (3D). Steel reinforcement was modeled using embedded truss elements (1D) with BJTS-420B material having a yield strength ($f_y$) of 420 MPa. The configuration of 12 D22 longitudinal

reinforcement was created according to Figure 1 with a concrete cover of 40 mm. All hoops and ties in a section were modeled in the same plane and without hooks. For simplification, hoops and ties outside the connection region were also modeled with a total of 4 legs in each direction, similar to those in the connection region, at 125 mm.

The contact interface between upper and lower column segments was modeled at a distance of 1 m from the fixed support at the column base. The steel plates at the ends of the column segments and the Ø150 mm × 10 mm steel pipe were not modeled because the contact and flush surfaces at the connection can be perfectly modeled in the finite element model. A Ø130 mm × 20 mm × 1200 mm steel pipe with a yield strength ($F_y$) of 550 MPa was modeled using solid elements (3D) as shown in Figure 2. Plain concrete was also modeled inside the pipe using solid elements (3D).

All concrete material was modeled with the concrete smeared crack model with a compressive strength ($f'_c$) of 35 MPa, modulus of elasticity of 27,805 MPa, and Poisson's ratio of 0.15 in unconfined condition. The steel reinforcement and pipe material were modeled using the isotropic–von Mises model, with a modulus of elasticity of 200 GPa and Poisson's ratio of 0.3. The bond between the concrete and the reinforcement and between the concrete and the steel pipe was assumed to be perfect. The concrete and the longitudinal reinforcements were made disconnected and without contact at the contact plane of the two column segments.

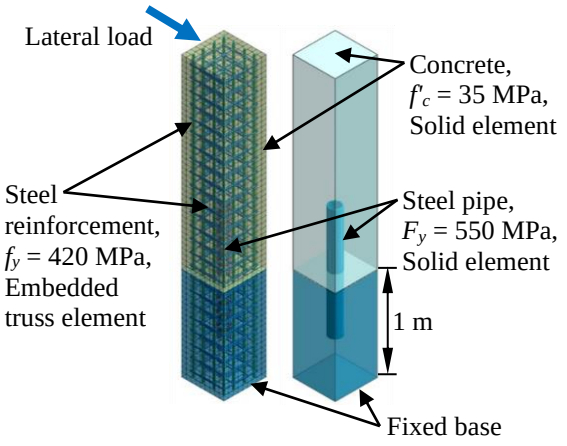


Fig.2 Finite element model of precast concrete column with mortise-tenon splice

A displacement-controlled monotonic lateral load was applied at the top of the column until a top column displacement (δ) of 50 mm was reached. Since the column cross-section is symmetrical, this lateral load was sufficiently applied to one face of the column and aligned with one of the principal axes of the column. Due to software limitations in MIDAS FEA NX, a constant axial load could not be applied simultaneously with the non-constant lateral load; therefore, no axial load was applied to the column model. This limitation means that tensile cracking may be overestimated and the results should be interpreted conservatively. The self-weight of the concrete and steel materials was also neglected to ensure no axial load effect in the analysis results. Load increments were automatically controlled by the solver with a maximum displacement step of 0.1 mm to capture nonlinear behavior accurately.

For comparison, a monolithic concrete column without a mortise-tenon splice was also modeled in MIDAS FEA NX in a manner similar to the precast concrete column with the mortise-tenon splice. In the monolithic column model, stirrups were modeled with a uniform spacing of 125 mm. Concrete and longitudinal reinforcement were made continuous from the base to the top of the column. Steel pipe was not modeled in the monolithic concrete column model.

## 4. RESULTS AND DISCUSSIONS

The crack pattern of the precast concrete column with a mortise-tenon splice is shown in Figure 3. Cracks in the concrete first appeared on the tension side at the column base and the connection, and continued to form on the tension side of the column. At approximately 9 mm displacement, cracks began to form on the compression side of the column. Cracks on the tension side continued to propagate upward away from the support, while cracks on the compression side only formed in the connection region. This crack distribution indicates that force transfer from the steel pipe to the lower column segment concentrates damage at the connection interface. At a displacement of 24.5 mm, most of the concrete in the connection region had cracked. From a displacement of 25 mm up to 50 mm, all concrete had cracked.

The crack pattern of the monolithic concrete column is shown in Figure 4. The first cracks appeared on the tension side at the column base and then propagated upward and toward the compression side of the column. From a displacement of 25 mm to 50 mm, cracks on the compression side had begun to form from the base of the column up to 0.5 m from the base. Because force and moment transfer along the monolithic column occurs more uniformly, the crack pattern follows the moment profile of the column and only

occurs on the tension side. This contrasts sharply with the precast column, where concentrated cracking or damage in the connection region confirms that the splice fundamentally alters the load path compared to monolithic construction.

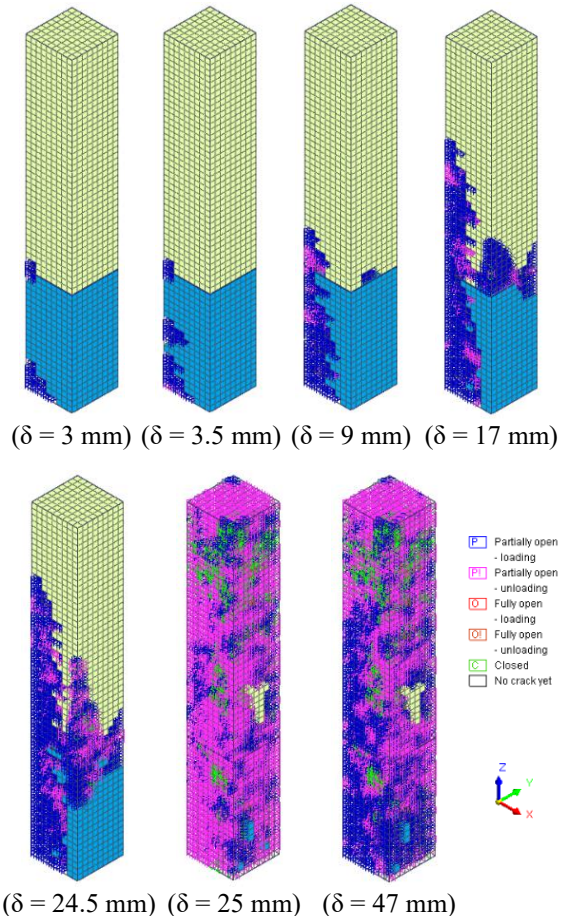


Fig.3 Crack pattern of precast concrete column with mortise-tenon splice

The axial stress of the longitudinal and transversal steel reinforcements is shown in Figure 5 for a top column displacement of 24 mm. In this figure, blue regions indicate high compressive stress and red regions indicate high tensile stress in the reinforcements. It can be seen that the maximum compressive stress in the longitudinal reinforcements and maximum tensile stress in the transverse reinforcements occur at the connection level, at the base of the upper column segment. This concentration of reinforcement stress at the connection interface, rather than at the column base where maximum moment occur in a monolithic column, confirms that the concrete-filled steel pipe acts as the primary load-transfer mechanism. The transverse reinforcement experiences increased tensile demand at this location, indicating that the pipe mobilizes the surrounding reinforcement but also creates a localized stress concentration at the connection level.

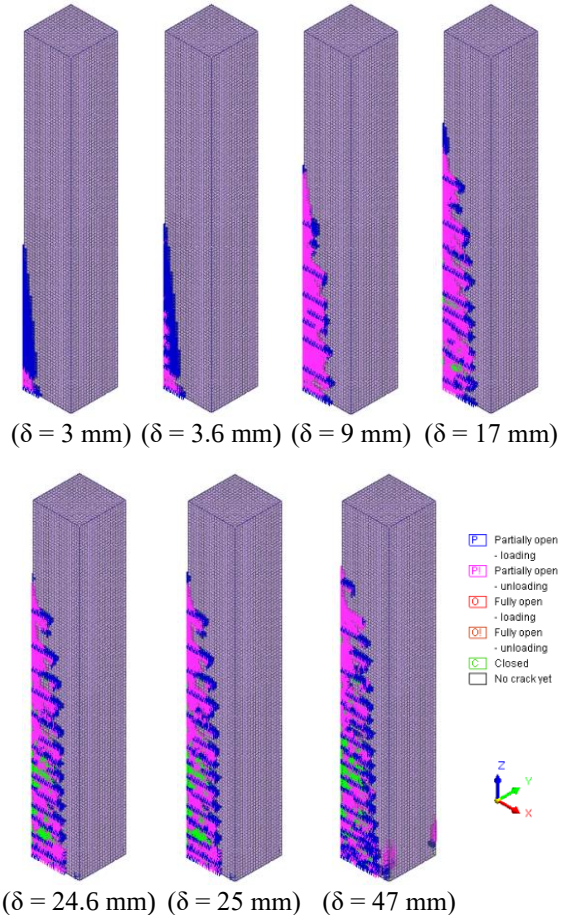


Fig.4 Crack pattern of monolithic concrete column

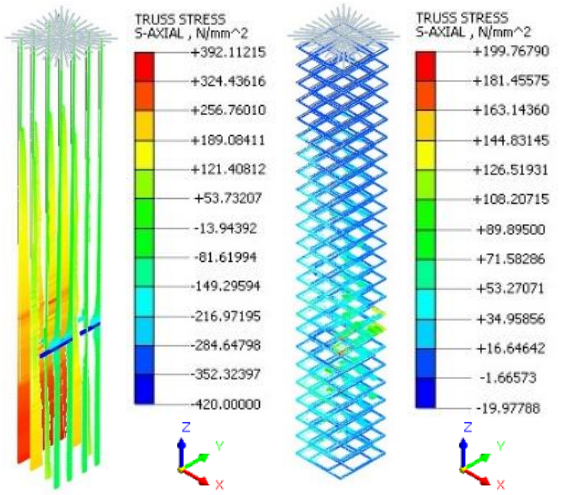


(a) Longitudinal reinforcement (b) Transversal reinforcement

Fig.5 Distribution of axial stress of reinforcements in precast concrete column at δ = 24 mm

This phenomenon is mainly caused by the significant force transfer between the pipe as the tenon component and the upper concrete column as the mortise component which makes the concrete in the compressive zone ineffective in resisting the internal forces.

The von Mises stress in the steel pipe used in the mortise-tenon splice of the precast concrete column is shown in Figure 6 and 7. Figure 6 presents the stress distribution across the entire pipe length, while Figure 7 plots the stress evolution at the critical connection interface as a function of displacement. The highest von Mises stress occurs at the interface between the upper and lower column segments, indicated by red color. A significant increase in von Mises stress begins at approximately 17 mm displacement, corresponding to the point at which extensive concrete cracking in the connection region transfers additional load to the steel pipe.

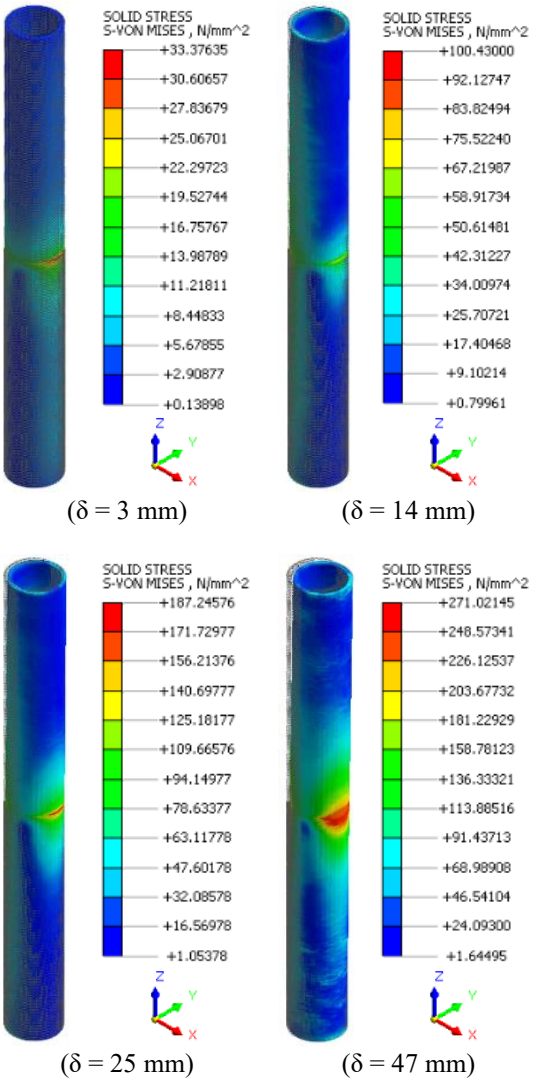


Fig.6 Distribution of von Mises stress of steel pipe in precast concrete column mortise-tenon splice

The load-displacement curves for the monolithic concrete column and for the precast concrete column with the mortise-tenon splice are shown in Figure 8. The precast concrete column with the mortise-tenon splice ("PC+MTSplice" line) exhibit similar curve shape to the monolithic concrete column, but with a lower load for a similar displacement. This reduction is attributed to early concrete cracking at the connection interface, which reduces stiffness before the steel pipe becomes fully mobilized.

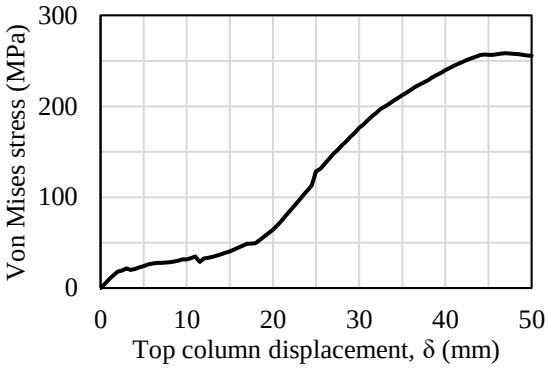


Fig.7 Von Mises stress curve of the steel pipe in the connection level

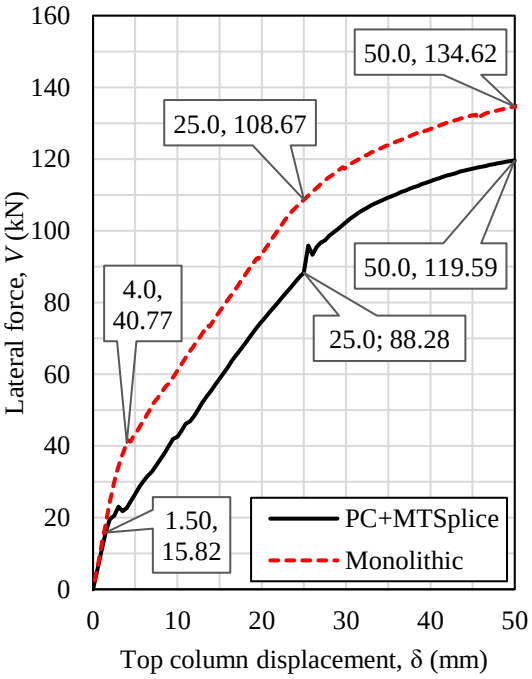


Fig.8 Lateral load-displacement curves for concrete columns with and without mortise-tenon splice

The first segment of the load-displacement curves represents the uncracked column condition up to a displacement of 1.5 mm with a lateral load of

15.82 kN for the precast concrete column and a displacement of 4 mm with a lateral load of 40.77 kN for the monolithic column. This difference occurs due to significant force transfer at the splice in the precast column. Even though the first segment ends at different points for these columns, the slope is similar for both columns.

The second segment of the curves have similar slope, which are 3.08 kN/mm for the precast concrete column and 3.23 kN/mm for the monolithic column. This slope is approximately equal to 30% of the first segment's slope. The reduction occurs because of the formation of numerous cracks along the column height until a top column displacement of 25 mm. The lateral force at this displacement value, which is 88.28 kN, is considered as the maximum lateral load that the precast concrete column can carry, as it indicates the condition where all concrete has cracked in the finite element model. The lateral load continues to increase due to the presence of the steel pipe until a displacement of 50 mm with a load of 119.59 kN for the precast concrete column.

The maximum lateral load was also calculated based on the rational design procedure provided by Jusuf et al. [24]. According to this design procedure, the precast concrete column with the mortise-tenon splice can carry a maximum factored lateral load of 60.95 kN. This value cannot be directly compared with the finite element analysis results because the analysis provides the nominal capacity of the model. The ratio of the maximum factored lateral load from the manual calculation to the nominal maximum lateral load from the finite element analysis is 0.69. This ratio does not exceed the strength reduction factor of 0.75 commonly used for concrete shear capacity. This result confirms that the design procedure by Jusuf et al. [24] yields conservative estimates and can be used as the rational design procedure required by the codes [12-13] for designing experimental specimens.

The moment-rotation relationship of the precast concrete column mortise-tenon splice is shown in Figure 9. The shape of the moment-rotation curve is similar to the load-displacement curve and can be simplified into a trilinear line. The intersection of the first and second segments of the trilinear line can be taken at a rotation of 0.28 mrad, corresponding to a top column displacement of 1 mm, and a bending moment of 21.53 kNm. The intersection of the second and third segments can be taken at a rotation of 6.89 mrad, corresponding to a top column displacement of 25 mm, and a bending moment of 176.55 kNm. This makes the slope of the first and second segments equal to 78,190 kNm/rad and 23,420 kNm/rad, respectively.

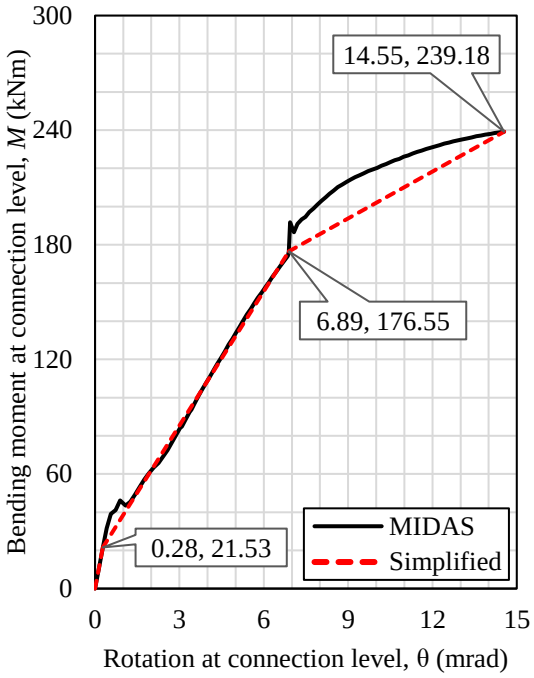


Fig.9 Moment-rotation curves of precast concrete column mortise-tenon splice

Based on Figure 9, the secant rotational stiffness of the connection can be determined as the ratio of the bending moment and the rotation at the connection. Under initial loading conditions, the connection has a secant rotational stiffness of 78,190 kNm/rad. At a rotation of 6.90 mrad, the secant rotational stiffness of the connection is 25,607 kNm/rad, or 33% of the initial rotational stiffness. At a rotation of 14.55 mrad, corresponding to a top column displacement of 50 mm, the secant rotational stiffness of the connection is 16,440 kNm/rad, or 21% of the initial rotational stiffness. These stiffness values provide quantitative benchmarks for engineers designing precast concrete moment frame buildings utilizing this connection type and are essential for determining seismic performance [26].

## 5. CONCLUSION

This study discusses the behavior of a precast concrete column mortise-tenon splice connection utilizing a concrete-filled steel pipe oriented parallel with the column longitudinal axis under monotonic lateral loading using the finite element method. The finite element analysis results show that the load-displacement curve of the precast concrete column with the mortise-tenon splice utilizing a concrete-filled steel pipe is similar in shape to that of a monolithic concrete column, but with a lower load. The difference occurs due to load transfer at the

mortise-tenon splice level that caused early cracking of the concrete, concentrating damage at the connection interface rather than distributing it along the column height as in monolithic construction.

The precast concrete column with the mortise-tenon splice under consideration has a lateral load capacity of 88.28 kN and a secant rotational stiffness of 25,607 kNm/rad at a top column displacement of 25 mm. These values represent the point at which concrete in the connection region has fully cracked, after which the steel pipe becomes the primary load-carrying mechanism. The rotational stiffness at this displacement is approximately 33% of the initial stiffness, providing quantitative data for seismic design applications.

For the precast concrete column with the mortise-tenon splice, the rational design procedure developed by Jusuf et al. [24] yields a factored lateral load capacity of 60.95 kN, which is 69% of the finite element analysis result. This ratio does not exceed the strength reduction factor of 0.75 commonly used for concrete shear capacity, confirming that the design procedure by Jusuf et al. [24] provides conservative results suitable for proportioning test specimens per code requirements [12-13].

This first numerical investigation of a mortise-tenon splice for precast concrete columns utilizing concrete-filled steel pipe has identified critical behavioral mechanisms that were not previously understood, including localized stress concentrations in reinforcement and concentrated damage at the connection interface. These findings provide essential pre-experimental insights that will aid specimen design and instrumentation planning for future laboratory testing.

This study is purely numerical and subject to simplifications including the absence of axial load and perfect bond assumptions. Therefore, experimental testing under both monotonic and cyclic loading remains necessary to verify the behavior of the mortise-tenon splice utilizing a concrete-filled steel pipe considered in this study. Future work should include full-scale cyclic testing to assess energy dissipation capacity, ductility, and seismic performance, as well as parametric studies to investigate the influence of pipe dimensions, concrete strength, and axial load levels.

## 6. ACKNOWLEDGMENTS

The authors would like to express their gratitude to Tarumanagara University for their support, PT Midasindo Teknik Utama for providing the licensed MIDAS FEA NX software used in this study, and to all parties that provided assistance in this study.

## 7. REFERENCES

1. Christianto, D., Makarim, C.A., Tavio, and Pratama, I.D., Modified EC2's Shear Strength Equation for No Coarse Aggregate RC Beams, International Journal on Advanced Science Engineering Information Technology, Vol. 12, Issue 6, 2022, pp. 2211–2216. https://doi.org/10.18517/ijaseit.12.6.15247
2. Christianto, D., Tavio, Pratama, I.D., and Liucius, Y.U., Effect of Longitudinal Bars on Shear Strength Prediction of High-Strength No-Coarse Aggregate Concrete, International Journal of Engineering Applications, Vol. 11, Issue 2, 2023, pp. 137–142. https://doi.org/10.15866/irea.v11i2.22596
3. Christianto, D., Makarim, C.A., and Tavio, Influence of Longitudinal Reinforcement Ratio on Shear Capacity of No Coarse-Aggregate Concrete, International Journal of GEOMATE, Vol. 21, Issue 86, 2021, pp. 122–130. https://doi.org/10.21660/2021.86.j2288
4. Christianto, D., Leman, S., Liucius, Y.U., Tavio, Ju, H., Nizam, Z.M., Jusuf, A.H., and Kho, D.A., Modified Reinforcement and Splitting Tensile Strength Factors in ACI 318 Shear Strength Formula for Concrete Without Coarse Aggregate, International Journal of Engineering Applications, Vol. 13, Issue 4, 2025, pp. 386–392. https://doi.org/10.15866/irea.v13i4.25209
5. Kushartomo, W., Wiyanto, H., and Christianto, D., Effect of Cement–Water Ratio on the Mechanical Properties of Reactive Powder Concrete with Marble Powder as Constituent Materials, In: Lie, H.A., Sutrisna, M., Prasetijo, J., Hadikusumo, B.H., and Putranto, L.S. (eds), Proceedings of the Second International Conference of Construction, Infrastructure, and Materials, Lecture Notes in Civil Engineering, Vol. 216, 2022, pp. 177–185. https://doi.org/10.1007/978-981-16-7949-0_16
6. Widjaja, W., Christianto, D., Kurniadi, D., Monica, L., Yuliana, and Michelle, Shear Capacity of Fiber-Reinforced Concrete Beams without Transverse Reinforcement, IOP Conference Series: Materials Science and Engineering, Vol. 650, 2019, Art. No. 012036. https://doi.org/10.1088/1757-899X/650/1/012036
7. Christianto, D., Tavio, and Irianto, M.R., Shear Strength of SFRC Beams Without Coarse Aggregate Using Finite Element Analysis with Bond-Slip, International Review of Civil Engineering, Vol. 14, Issue 4, 2023, pp. 320–330. https://doi.org/10.15866/irece.v14i4.22482
8. Sanjaya, A., Tavio, and Christianto, D., Experimental Study of Mortar Compressive Strength with Anadara Granosa Powder as a Substitute for Partial Use of Cement, IOP Conference Series: Materials Science and Engineering, Vol. 650, 2019, Art. No. 012037.

https://doi.org/10.1088/1757-899X/650/1/012037
9. Kurama, Y.C., Sritharan, S., Fleischman, R.B., Restrepo, J.I., Henry, R.S., Cleland, N.M., Ghosh, S.K., and Bonelli, P., Seismic-Resistant Precast Concrete Structures - State of the Art, Journal of Structural Engineering, Vol. 144, Issue 4, 2018, Article 03118001. https://doi.org/10.1061/(ASCE)ST.1943-541X.0001972
10. fib Commission 7, Seismic Design of Precast Concrete Building Structures (fib Bulletin 27), International Federation for Structural Concrete, 2003, pp. 1–262. https://doi.org/10.35789/fib.BULL.0027
11. Wong, R.W.M., and Loo, B.P.Y., Sustainability Implications of Using Precast Concrete in Construction: An In-Depth Project-Level Analysis Spanning Two Decades. Journal of Cleaner Production, Vol. 378, 2022, Art. No. 134486. https://doi.org/10.1016/j.jclepro.2022.134486
12. ACI Committee 318, Building Code Requirements for Structural Concrete (ACI 318-19), American Concrete Institute, 2019, pp. 1–624. https://doi.org/10.14359/51716937
13. ACI Committee 374, Acceptance Criteria for Moment Frame Based on Structural Testing and Commentary (ACI 374.1-05), American Concrete Institute, 2005, pp. 1–9.
14. Hansapinyo, C., Siri, N., and Buachart, C., Capacity Design Criteria for Seismic Resistance of Precast Concrete Columns Using Steel Box Connection, International Journal of GEOMATE, Vol. 14, Issue 45, 2018, pp. 1–9. https://doi.org/10.21660/2018.45.7360
15. Nzabonimpa, J.D., and Hong, W.K., Experimental and Nonlinear Numerical Analysis of Precast Concrete Column Splices with High-Yield Metal Plates, Journal of Structural Engineering, Vol. 145, Issue 2, 2019, Art. No. 04018254. https://doi.org/10.1061/(ASCE)ST.1943-541X.0002233
16. Nguyen, D.H. and Hong, W.K., Nonlinear Finite Element Analysis of Mechanical Connections Splicing Precast Columns with Stiffened Laminated Metal Plates, Journal of Asian Architecture and Building Engineering, Vol. 19, Issue 6, 2020, pp. 670–699. https://doi.org/10.1080/13467581.2020.1775604
17. Yan, J. and Jiang, L., Research on the Seismic Performance of the Prefabricated Reinforced Concrete Column with Steel Mortise and Tenon Connections, Advances in Civil Engineering, Vol. 2021, 2021, Art. No. 6675231. https://doi.org/10.1155/2021/6675231
18. Prasetya, D. K. and Tavio, Innovative Bolted-Steel Box for Seismic-Resistant Dry-Precast Concrete Beam-Column Connection, 2022, IOP Conference Series: Earth and Environmental Science, Volume 1116, 2022, Art. No. 012012. https://doi.org/10.1088/1755-1315/1116/1/012012
19. Zhu, Z., Wu, F., and Hao, J., Mechanical Behavior of a Novel Precast Concrete Beam-Column Joint Using the Mortise-Tenon Connection, Sustainability, Vol. 15, Issue 19, 2023, Art. No. 14586. https://doi.org/10.3390/su151914586
20. Wang, J., Zhang, W., and Zhang, C., The Cyclic Performance and Macro-Simplified Analytical Model of Internal Joints in RC-Assembled Frame Structures Connected by Unbonded Prestressed Strands and Mortise-Tenon Based on Numerical Studies, Buildings, Vol. 14, Issue 6, 2024, Art. No. 1629. https://doi.org/10.3390/buildings14061629
21. Siswosukarto, S., Setiawan, A.F., Darmawan, M.F., Muflikhun, M.A., and Faveryan, B., Experimental and Numerical Simulation of GFRP Confined Cylindrical Concrete Under Compression, International Journal of GEOMATE, Vol. 27, Issue 119, 2024, pp. 50–58. https://doi.org/10.21660/2024.119.4374
22. Sandjaya, A., Alisjahbana, S.W., Suryoatmono, B., and Prabowo, A., Post-Buckling Behavior of Cold-Formed Steel Square Plate Fixed Supported Under Pure Shear, International Journal of GEOMATE, Vol. 29, Issue 133, 2025, pp. 81–88. https://doi.org/10.21660/2025.133.5023
23. Akhmad, R.H.P. and Tavio, Influence of Seawater on Strength of Concrete Beams Strengthened with Glass Fiber Reinforced Polymer Sheet, International Journal of GEOMATE, Vol. 26, Issue 117, 2024, pp. 35–42. https://doi.org/10.21660/2024.117.4330
24. Jusuf, A.H., Christianto, D., Pranoto, W.A., Leman, S., and Tavio, Analisis Sambungan Mortise-Tenon Kolom Beton Pracetak dengan Pipa Baja Diisi Beton [Analysis of Precast Concrete Column Mortise-Tenon Connection with Concrete-Filled Steel Pipe], Jurnal Teknik Sipil, Vol. 17, Issue 4, 2024, pp. 277–288. https://doi.org/10.24002/jts.v17i4.10119
25. Osanai, Y., Watanabe, F., and Okamoto, S., Stress Transfer Mechanism of Socket Base Connections with Precast Concrete Columns, ACI Structural Journal, Vol. 93, Issue 3, 1996, pp. 266–276. https://doi.org/10.14359/9686
26. Liucius, Y.U. and Jovan, A., Analysis of Ductility Parameters and Building Performance Level on Dual System Structure Retrofitted with Steel Bracing, E3S Web of Conferences, Vol. 429, 2023, Art. No. 05025. https://doi.org/10.1051/e3sconf/202342905025